Revista Mexicana de Astronomía y Astrofísica, **39**, 261–266 (2003)

AN ANALYTIC MODEL FOR THE MOTION OF THE HEAD OF A VARIABLE JET

J. Cantó[1] and A. C. Raga[2]

Received 2003 May 27; accepted 2003 June 30

RESUMEN

Presentamos un modelo para el movimiento de la cabeza de un jet variable que conserva tanto masa como momento. Nuestro modelo en principio se puede aplicar a una variabilidad arbitraria. Sin embargo, presentamos soluciones completas sólo en dos casos: "variabilidad sinusoidal de velocidad + pérdida de masa constante" y "variabilidad sinusoidal de velocidad + densidad de eyección constante".

ABSTRACT

We present a model for the motion of the head of a variable jet which conserves both mass and momentum. Our model is in principle applicable for an ejection variability of arbitrary form. However, we present full solutions for only two cases: "sinusoidal velocity variability + constant mass loss rate" and "sinusoidal velocity variability + constant ejection density".

Key Words: **ISM: HERBIG-HARO OBJECTS — ISM: JETS AND OUTFLOWS — ISM: KINEMATICS AND DYNAMICS**

1. INTRODUCTION

The problem of the formation and the motion of working surfaces in a hypersonic, variable jet is simple enough that it can be attacked with analytic methods. Past efforts in this direction have had varying degrees of success, and have been based on two possible approaches, which we describe below.

In a hypersonic jet ejected with a time-dependent velocity, pairs of shocks ("internal working surfaces") form, and travel down the jet flow (Raga et al. 1990). The continuous segments in between the working surfaces are "ballistic" (i.e., as the flow is hypersonic, the pressure is negligible), and preserve the flow velocity with which the material was ejected from the source. For these ballistic segments, the continuity equation has an exact, analytic integral (Raga & Kofman 1992), so that there is a full analytic solution for the flow within the continuous jet beam segments.

The working surfaces are produced when faster material collides either with the surrounding environment (at the head of the jet) or with slower material ejected previously from the jet source (at the internal working surfaces). The full solution for the jet flow is then obtained by "patching" the free-streaming solution for the continuous segments with the equations of motion for the successive working surfaces.

There are two possible equations of motion that can be considered for the working surfaces:

- the equation resulting from the ram pressure balance condition across the two working surface shocks,
- the equation for the motion of the center of mass of the material within the working surface.

The first of these two possibilities represents the motion of a working surface that rapidly loses mass sideways into a cocoon (surrounding the jet beam), so that the inertia of the material within the working surface is negligible. The second model corresponds to a working surface which conserves (within the region in between the two shocks) most of the mass that has gone through the working surface shocks. It has been shown (Masciadri et al. 2002) that numerical simulations of variable jets give results that lie in between these two ("massless" or "mass conserving" working surface) assumptions.

The first efforts to obtain analytic models were based on the "massless working surface" assumption, and were calculated with a constant density approximation for the gas in the jet beam (Raga et al. 1990).

[1]Instituto de Astronomía, Universidad Nacional Autónoma de México, México, D. F., México.

[2]Instituto de Ciencias Nucleares, Universidad Nacional Autónoma de México, México, D. F., México.

Kofman & Raga (1992) and Raga & Kofman (1992) derived an asymptotic solution for long distances from the source, valid for an arbitrary velocity and density ejection variability. Raga & Cantó (1998) considered the exact solution to the "free streaming flow + massless working surface" problem, but were unable to solve the differential equations of motion of the working surfaces in an analytic way.

Cantó, Raga, & D'Alessio (2000) first studied solutions to the "mass conserving working surface" problem. They showed that the position of the working surface has to coincide with the position of the center of mass of all of the material confined between the two working surface shocks. This condition leads to an integral formalism, which gives complex but tractable analytic solutions. Cantó et al. (2000) computed the solution for the "free streaming flow + mass conserving working surface" problem for the case of a sinusoidally varying ejection velocity (with either a constant mass loss rate or constant ejection density).

In a recent paper, Raga & Cantó (2003) have developed an analytic model for the motion of the leading head of a variable jet. In this model, the head travels forward (sweeping up environmental material) and is impacted from behind by the successive "pulses" of material (corresponding to the internal working surfaces, which are assumed to concentrate all of the material ejected from the source). The model of Raga & Cantó (2003) has the limitation that the jet is assumed to be composed of a series of travelling "clumps", but is missing a calculation of the concentration of the jet beam material into the successive working surfaces.

In the present paper, we discuss a full model for the head of a jet from a variable source, in which we consider the details of the time-dependence of the ejection. This model incorporates both the concentration of the jet material into a series of internal working surfaces, as well as the impacts of the working surfaces as they catch up with the leading head of the jet.

The general formalism of the analytic model is dicussed in § 2. In § 3, we present the solutions obtained for a sinusoidally varying velocity and with either a constant mass loss rate or constant ejection density. Finally, we discuss the results in § 4.

2. THE ANALYTIC MODEL

We consider the motion of the head of a variable jet, which is ejected with a time-dependent mass loss rate $\dot{m}(\tau)$ (per unit area of the jet) and velocity $v_{\rm i}(\tau)$, where τ is the time at which the material is being ejected. We will assume that the ejection starts at $\tau = 0$, producing a jet that is moving into an undisturbed, stationary environment.

If we assume that the jet is perfectly collimated (i.e., that it has zero opening angle) and that all of the material intercepted by the head of the jet remains within it, the mass (per unit area of the jet cross section) of the jet head is given by

$$m_{\rm s} = \int_0^{x_{\rm s}} \rho_{\rm e}\, dx + \int_0^{\tau_{\rm s}} \dot{m}(\tau)\, d\tau, \qquad (1)$$

where $x_{\rm s}$ is the position of the head of the jet, $\rho_{\rm e}$ is the environmental density and $\tau_{\rm s}$ is the time at which the material which is now just catching up with the working surface was ejected from the source.

The momentum (per unit area) of the head of the jet is

$$\Pi_{\rm s} = \int_0^{\tau_{\rm s}} \dot{m}(\tau)\, v_{\rm i}(\tau)\, d\tau. \qquad (2)$$

The velocity of the jet head is then

$$v_{\rm s} = \Pi_{\rm s}/m_{\rm s}. \qquad (3)$$

The position of the head of the jet $x_{\rm s}$ can be computed as the position of the center of mass of the swept up environment and the jet material (ejected between times 0 and $\tau_{\rm s}$) that has caught up with the jet head:

$$x_{\rm s} = \frac{1}{m_{\rm s}} \left[\int_0^{x_{\rm s}} \rho_{\rm e} x\, dx + \int_0^{\tau_{\rm s}} (t-\tau)\, \dot{m}(\tau)\, v_{\rm i}(\tau)\, d\tau \right]. \qquad (4)$$

The position of the head also satisfies the condition

$$x_{\rm s} = (t-\tau_{\rm s})\, v_{\rm i}(\tau_{\rm s}) \quad \rightarrow \quad t = \frac{x_{\rm s}}{v_{\rm i}(\tau_{\rm s})} + \tau_{\rm s}, \qquad (5)$$

namely, that the material ejected from the source at a time $\tau_{\rm s}$, travelling with a ballistic velocity $v_{\rm i}(\tau_{\rm s})$ is now (i.e., at time t) just catching up with the head of the jet. It will be shown below that the ejection velocity $v_{\rm i}(\tau_{\rm s})$ and time $\tau_{\rm s}$ change discontinuously each time an internal working surface impacts the head. These changes, however, are such that equation (5) is still valid at any time, since the position of the head $x_{\rm s}$ must be a continuous function of time.

For a uniform environment, $\rho_{\rm e}$ is independent of x, and the first integral in equation (1) is equal to $\rho_{\rm e}\, x$. Substituting equation (1) into (4) we then obtain a quadratic equation for $x_{\rm s}$:

$$\frac{\rho_{\rm e}}{2} {x_{\rm s}}^2 + A(\tau_{\rm s})\, x_{\rm s} + B(\tau_{\rm s}) = 0, \qquad (6)$$

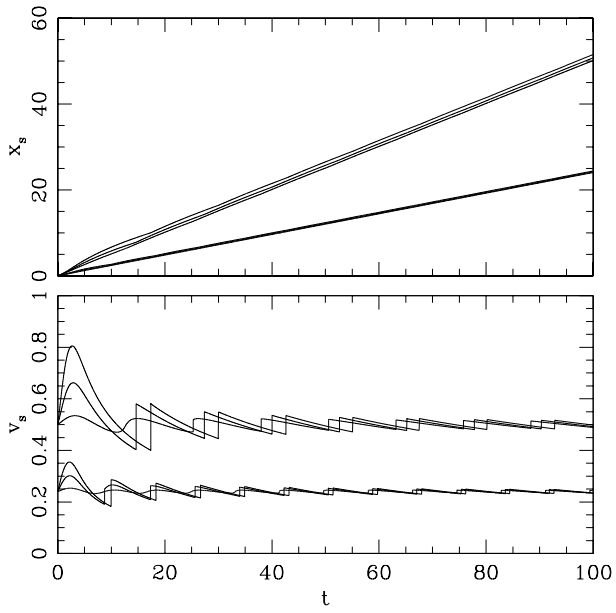

Fig. 1. Position x_s (top) and velocity v_s (bottom) of the head of the jet as a function of time t obtained from the "sinusoidal ejection velocity + constant mass loss rate" model (see § 3.1). Six choices of parameters are shown. In both plots the three upper curves correspond to $\rho_e = 1$, and the three lower curves to $\rho_e = 10$. Of each of the groups of three curves, the curve with larger values of x_s and larger variability in v_s corresponds to $v_a = 1.0$. The two other curves correspond to $v_a = 0.5$ and $v_a = 0.1$ (which gives the lower values for x_s and for the variability of v_s).

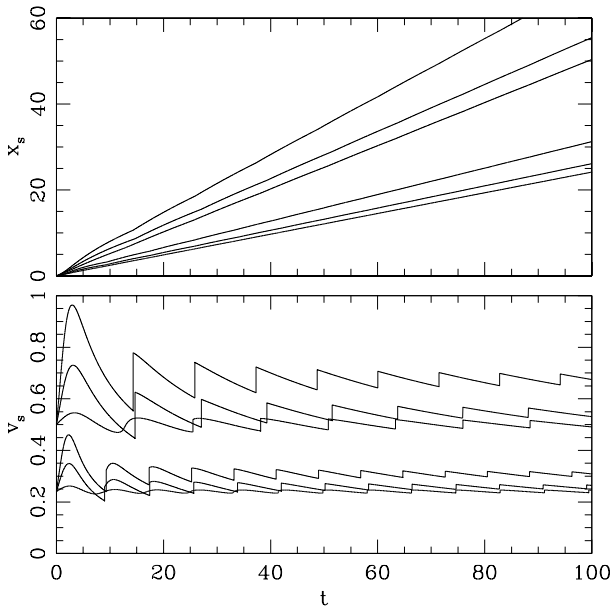

Fig. 2. Position x_s (top) and velocity v_s (bottom) of the head of the jet as a function of time t obtained from the "sinusoidal ejection velocity + constant ejection density" model (see § 3.2). Six choices of parameters are shown. In both plots the three upper curves correspond to $\rho_e = 1$, and the three lower curves to $\rho_e = 10$. Of each of the groups of three curves, the curve with larger values of x_s and larger variability in v_s corresponds to $v_a = 1.0$. The two other curves correspond to $v_a = 0.5$ and $v_a = 0.1$ (which gives the lower values for x_s and for the variability of v_s).

where

$$A(\tau_s) \equiv \int_0^{\tau_s} \dot{m}(\tau)\, d\tau - \frac{1}{v_i(\tau_s)} \int_0^{\tau_s} \dot{m}(\tau)\, v_i(\tau)\, d\tau, \quad (7)$$

$$B(\tau_s) = -\tau_s \int_0^{\tau_s} \dot{m}(\tau)\, v_i(\tau)\, d\tau + \int_0^{\tau_s} \dot{m}(\tau)\, v_i(\tau)\, \tau\, d\tau. \quad (8)$$

Given the functional forms of $\dot{m}(\tau)$ and $v_i(\tau)$, we can use equations (7) and (8) to find $A(\tau_s)$ and $B(\tau_s)$, and solve the quadratic equation (6) in order to find x_s. We can then obtain the time t from equation (5), and the velocity v_s of the head of the jet from equations (1–3). In this way, we obtain the position x_s and the velocity v_s of the head of the jet as a function of time t in a parametric way, by computing the values of x_s, v_s and t corresponding to all of the positive values of the parameter τ_s. This procedure is illustrated in the following section for specific forms of $\dot{m}(\tau)$ and $v_i(\tau)$.

3. THE CASE OF A SINUSOIDAL EJECTION VELOCITY

3.1. *Constant Mass Loss Rate*

Let us now consider an ejection variability of the form:

$$\dot{m}(\tau) = 1, \quad v_i(\tau) = 1 + v_a \sin\tau, \quad (9)$$

where v_a is the (dimensionless) amplitude of the velocity variability. This dimensionless form is obtained by writing the time τ in units of $\tau_0/2\pi$ (where τ_0 is the dimensional period of the variability), the velocities in units of v_0 (the average, dimensional ejection velocity) and the densities in units of ρ_0 (the average, dimensional ejection density). In the dimensionless form of equation (9), both the total mass m_0 and momentum Π_0 ejected in one variability period are equal to 2π.

Substituting equation (9) into (7–8), one obtains

$$A(\tau_s) = v_a \frac{\cos\tau_s + \tau_s \sin\tau_s - 1}{1 + v_a \sin\tau_s}, \quad (10)$$

$$B(\tau_s) = -\frac{1}{2}\tau_s(\tau_s + 2v_a) + v_a \sin\tau_s. \quad (11)$$

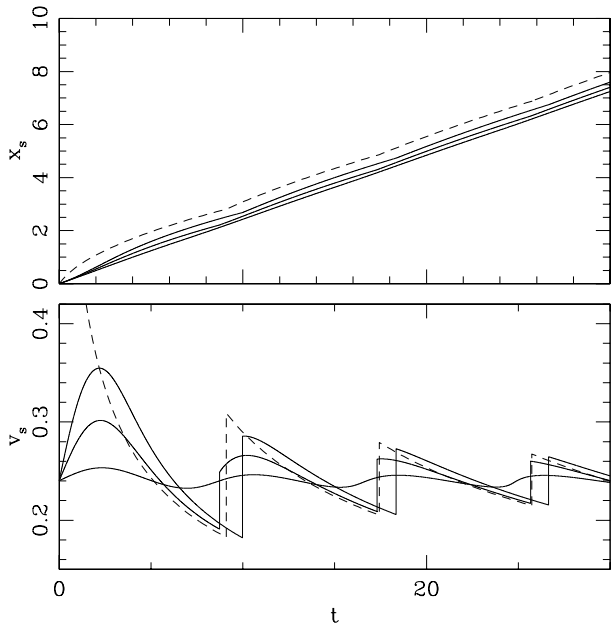

Fig. 3. Comparison between our "sinusoidal ejection velocity + constant mass loss rate" model and the "discrete pulse" model of Raga & Cantó (2003). The three solid curves correspond to parameters $\rho_{\rm e} = 10$ and $v_{\rm a} = 1.0$, 0.5 and 0.1, and the dashed curve corresponds to the model of Raga & Cantó (2003) with $\rho_{\rm e} = 10$.

The solution to the quadratic equation (6) then gives the position as a function of $\tau_{\rm s}$. The velocity of the jet head is given by equation (3) which now takes the form

$$v_{\rm s} = \frac{\tau_{\rm s} + v_{\rm a}(1 - \cos\tau_{\rm s})}{\rho_0 x_{\rm s} + \tau_{\rm s}}, \qquad (12)$$

and the time t as a function of $\tau_{\rm s}$ is finally obtained from equation (5).

From this parametric solution, we find, e.g., the position $x_{\rm s}$ of the jet head as a function of the time t. Interestingly, this is a multivalued function, with several different possible values of $x_{\rm s}$ for each value of t. One can show that the physical solution giving the real position of the jet head corresponds to the solution with the maximum value of $x_{\rm s}$ for each given time t.

In this way, we can fix different values of the dimensionless velocity amplitude $v_{\rm a}$ and environmental density $\rho_{\rm e}$, and then obtain the position $x_{\rm s}$ and velocity $v_{\rm s}$ of the jet head as a function of time. Several examples of such solutions are shown in Figure 1.

3.2. *Constant Ejection Density*

We now consider an ejection variability of the form:

$$\dot m(\tau) = 1 + v_{\rm a}\sin\tau, \quad v_{\rm i}(\tau) = 1 + v_{\rm a}\sin\tau, \qquad (13)$$

In this dimensionless form the total mass ejected in one variability period is $m_0 = 2\pi$, and the total momentum is $\Pi_0 = 2\pi(1 + {v_{\rm a}}^2/2)$.

Substituting equation (13) into (7–8), one obtains

$$A(\tau_{\rm s}) = -\frac{v_{\rm a}}{2(1 + v_{\rm a}\sin\tau_{\rm s})} \times \Big[2 + v_{\rm a}\,\tau_{\rm s} - 2(\tau_{\rm s} + v_{\rm a})\sin\tau_{\rm s} + \cos\tau_{\rm s}(-2 + v_{\rm a}\sin\tau_{\rm s})\Big], \qquad (14)$$

$$B(\tau_{\rm s}) = \frac{1}{8}\Big[-4{\tau_{\rm s}}^2 + 16 v_{\rm a}(\sin\tau_{\rm s} - \tau_{\rm s}) + {v_{\rm a}}^2(1 - 2{\tau_{\rm s}}^2 - \cos 2\tau_{\rm s})\Big]. \qquad (15)$$

Equation (3) for the velocity of the jet head now takes the form

$$v_{\rm s} = \frac{\tau_{\rm s} + 2v_{\rm a}(1 - \cos\tau_{\rm s}) + \frac{1}{2}{v_{\rm a}}^2(\tau_{\rm s} - \frac{1}{2}\sin 2\tau_{\rm s})}{\rho_0 x_{\rm s} + \tau_{\rm s} + v_{\rm a}(1 - \cos\tau_{\rm s})}. \qquad (16)$$

Solving equation (6) we then obtain the solution for the motion of the jet head as a function of time (choosing the appropriate solution for the multivalued function, as described in § 3.1).

In Figure 2, we show the position $x_{\rm s}$ and the velocity $v_{\rm s}$ as a function of time obtained for different values of $v_{\rm a}$ and $\rho_{\rm e}$. The results are discussed in the following section.

3.3. *Discussion*

In § 3.1 and § 3.2 we presented the solutions obtained for a sinusoidal velocity variability and a constant mass loss rate or a constant ejection density. Numerical examples of the results that are obtained are shown in Figs. 1 and 2.

From these figures it is clear that qualitatively similar results are obtained for the two cases. Initially, the jet head velocity $v_{\rm s}$ first increases (as a result of the initially increasing ejection velocity, see equations 9 and 13), reaches a peak, and then starts to decrease. This decrease in $v_{\rm s}$ is a direct result of the decrease of the ejection velocity beyond the first peak of the sinusoidal variability, together with the increase of the mass of the swept-up environmental material.

The velocity $v_{\rm s}$ then shows a number of oscillations, with increases at the times at which the head of the jet is caught up by the successive "ejection events" of the sinusoidal ejection velocity variability. From Figs. 1 and 2 it is clear that these increases are discontinuous for the $v_{\rm a} = 1.0$ and 0.5 cases, but are

first continuous (for $t < 50$) and then discontinuous (for $t > 50$) for the $v_a = 0.1$ model. This result is due to the following effect.

For large amplitudes, a sinusoidal velocity variability leads to the formation of internal working surfaces close to the jet source (the exact expression for the time and distance at which the working surfaces form is given by Raga & Noriega-Crespo 1998). Because of this, by the time that the second "ejection event" catches up with the jet head it has already steepened into an internal working surface, therefore giving a sudden boost to the momentum (and therefore to the velocity) of the jet head. This is what is occurring in the $v_a = 1.0$ and 0.5 models.

In the $v_a = 0.1$ model, the first few ejection events catch up with the jet head before they have steepened into internal working surfaces, and they therefore do not give such sudden boosts to the velocity of the jet head. However, at large enough distances from the source, they do form internal working surfaces, and start to produce discontinuous jumps in v_s when they catch up with the jet head.

It is interesting to compare our present results with the "discrete" model of Raga & Cantó (2003). These authors considered the motion of the head of a variable jet, which is formed of a periodic series of discrete "ejection events" of mass m_0 and momentum Π_0. In Figure 3, we show solutions for $\rho_e = 10$ and $v_a = 0.1$, 0.5 and 1.0 from our "constant mass loss rate" solution (see § 3.1), together with the solution from the "discrete" model of Raga & Cantó (2003) with the same values of m_0 and Π_0 (i.e., with the same mass and momentum per ejection event).

From Fig. 3, we see that for $t > 10$ the $v_a = 1.0$ and 0.5 solutions quite closely resemble the "discrete" model of Raga & Cantó (2003). However, the $v_a = 0.1$ model does not develop discontinuities (in v_s vs. t) in the time-range shown in Fig. 3, and therefore shows a qualitatively different behaviour.

It is mathematically interesting that the "continuous flow" model described in the present paper automatically develops the "discrete" behaviour of the model of Raga & Cantó (2003), which has this discreteness imposed in the form of the ejection time-variability. Even though the solutions for v_s that we obtain for the flow velocity are continuous as a function of τ_s (see equations 12 and 16), they do show discontinuities when plotted as a function of time t. These discontinuities result from the fact that one has to choose between the different branches of the $x_s(t)$ function (in which the branch with larger value of x_s represents the physical solution, see § 3.1 and § 3.2). The discontinuities in v_s correspond to the points in which one branch crosses another one, and suddenly becomes the solution with larger x_s (i.e., the physical solution).

From Fig. 3, we see that our model results in the same asymptotic velocity (for large times) as the discrete model of Raga & Cantó (2003), so we do not rederive its value here.

4. CONCLUSIONS

In this paper we derive a fully analytic model for the motion of the head of a variable jet, based on mass and momentum conservation considerations. This model is in principle applicable for an arbitrary ejection velocity and density variability, but we present explicit solutions for only two kinds of variabilities:

- sinusoidal velocity variability, constant mass loss rate,
- sinusoidal velocity variability, constant ejection density.

However, as our solution only involves integrals of the mass and momentum injection rates, any time-variability which leads to analytic forms for the relevant integrals (see equations 7 and 8) will lead to a full analytic solution.

We have only considered the case of a homogeneous, constant ρ_e environment. One could of course also consider the case of a stratified environment. However, most possible forms for the density stratification will lead to a transcendental equation for x_s as a function of τ_s (see equation 6), which would then require a numerical inversion. Also, in the present paper we have considered a perfectly collimated jet, but the case of a jet with a constant opening angle could also be treated with the same formalism (this would lead to a quartic equation for x_s as a function of τ_s).

This paper represents an extension to the work of Raga & Cantó (2003). These authors derived the motion of the head of a jet composed of a series of discrete "pulses" of mass m_0 and momentum Π_0. Our present model is much more general, as it represents a solution for an ejection variability of arbitrary form.

As discussed by Raga & Cantó (2003), this model for the motion of the head of a variable jet has clear applications for HH jets. For example, in young outflow systems one might be observing the leading head of a jet as it begins to escape from the dense region close to the source. An example of this kind of

flow might be the emission knots close to XZ Tauri (Krist et al. 1997), which appear to represent the initial stages of an outflow from a young star. Another example of an outflow in the initial stages of its evolution might be HH 57 (Reipurth et al. 1997). Also, our model could be applied to the leading head of an evolved outflow. Such leading heads might be associated with the knots farther away from the source in "giant jets" systems such as the ones associated with the HH 34 (Devine et al. 1997) and HH 111 (Reipurth, Bally, & Devine 1997) outflows.

We would like to acknowledge support from the CONACyT grants 36572-E and 41320 and the DGAPA (UNAM) grant IN 112602.

REFERENCES

Cantó, J., Raga, A. C., & D'Alessio, P. 2000, MNRAS, 313, 656
Devine, D., Bally, J., Reipurth, B., & Heathcote, S. 1997, AJ, 114, 2095
Kofman, L., & Raga, A. C. 1992, ApJ, 390, 359
Krist, J. E., Burrows, C. J., Stapelfeldt, K. R., et al. 1997, ApJ, 481, 447
Masciadri, E., Velázquez, P. F., Raga, A. C., Cantó, J., & Noriega-Crespo, A. 2002, ApJ, 573, 260
Raga, A., & Cantó, J. 2003, A&A, submitted
_____. 1998, RevMexAA, 34, 73
Raga, A. C., Cantó, J., Binette, L., & Calvet, N. 1990, ApJ, 364, 601
Raga, A. C., & Kofman, L. 1992, ApJ, 386, 222
Raga, A. C., & Noriega-Crespo, A. 1998, AJ, 116, 2943
Reipurth, B., Bally, J., & Devine, D. 1997, AJ, 114, 2708
Reipurth, B., Olberg, M., Gredel, R., & Booth, R. S. 1997, A&A, 327, 1164

Jorge Cantó: Instituto de Astronomía, UNAM, Apartado Postal 70-264, 04510 México, D. F., México.
Alejandro C. Raga: Instituto de Ciencias Nucleares, UNAM, Apartado Postal 70-543, 04510 Néxico, D. F., México. (raga@nuclecu.unam.mx).